CHIN. PHYS. LETT. Vol. 38, No. 7 (2021) 077401

Preparation of Superconducting Thin Films of Infinite-Layer Nickelate $Nd_{0.8}Sr_{0.2}NiO_2$

Qiang Gao(高强)[1], Yuchen Zhao(赵宇辰)[1,2], Xing-Jiang Zhou(周兴江)[1,2,3,4*], and Zhihai Zhu(朱志海)[1,2*]

[1]*National Lab for Superconductivity, Beijing National laboratory for Condensed Matter Physics, Institute of Physics, Chinese Academy of Sciences, Beijing 100190, China*
[2]*School of Physical Sciences, University of Chinese Academy of Sciences, Beijing 100049, China*
[3]*Beijing Academy of Quantum Information Sciences, Beijing 100193, China*
[4]*Songshan Lake Materials Laboratory, Dongguan 523808, China*

(Received 2 March 2021; accepted 17 May 2021; published online 21 June 2021)

The recent observation of superconductivity in thin films of infinite-layer nickelate $Nd_{0.8}Sr_{0.2}NiO_2$ has received considerable attention. Despite the many efforts to understand the superconductivity in infinite-layer nickelates, a consensus on the underlying mechanism for the superconductivity has yet to be reached, partly owing to the challenges with the material synthesis. Here, we report the successful growth of superconducting infinite-layer $Nd_{0.8}Sr_{0.2}NiO_2$ films by pulsed laser deposition and soft chemical reduction. The details on the growth process are discussed.

DOI: 10.1088/0256-307X/38/7/077401

Despite decades of research on cuprate superconductors, an understanding of what exact features of a material essentially support superconductivity has remained elusive. On an empirical basis, it seems natural to expect that superconductivity can be achieved through the synthesis of cuprate analogs that share common features including spin one-half, two-dimensionality, and strong antiferromagnetic correlations.[1] Along this direction, Chaloupka *et al.* proposed that $LaNiO_3/LaMO_3$ (M stands for a trivalent cation Al, Ga, etc.) superlattices would create superconductivity, which however has not been realized to date although the nickel-oxide superlattices have been successfully synthesized.[2] The recent report of superconductivity in an infinite-layer nickelate $Nd_{0.8}Sr_{0.2}NiO_2$ has opened an alternative route to achieve superconductivity in transition metal oxide materials in addition to cuprates.[3] Compared with cuprates, the superconducting nickelates comprise a similar two-dimensional (2D) square lattice, isoelectronic $3d^9$ valence state, and a superconducting dome in the phase diagram.[4–9] However, in sharp contrast to cuprates, the parent compound $NdNiO_2$ of superconducting nickelates does not exhibit any magnetic order down to 1.7 K,[10] indicating that the underlying superconducting mechanism differs from that of cuprate superconductors for which magnetisms are generally believed to be crucial for mediating Cooper pairs. Although various theoretical models have been proposed to explain the superconductivity in the superconducting nickelates,[11–50] a consensus model has not yet reached partly owing to the challenges with the synthesis, and only very few reports exist on achieving superconducting films of infinite-layer nickelates.[3,5,51–56] At present, superconductivity has not been observed in bulk $Nd_{1-x}Sr_xNiO_2$.[57–60]

In this Letter, we report the successful growth of superconducting infinite-layer $Nd_{0.8}Sr_{0.2}NiO_2$ films. The perovskite precursor phase nickelate films were prepared using pulsed laser deposition (PLD). The infinite-layer phase was acquired by a soft-chemistry reduction method. The thickness and out-plane x-ray diffraction (XRD) pattern of the prepared films were examined using a SmartLab x-ray diffractometer. The superconductivity was confirmed by transport measurements using a Quantum Design physical property measurement system (PPMS) with a standard four-probe configuration. The wire connection was made by melting indium.

The laser target contained a stoichiometric mixture of $SrCO_3$ (Alfa Aesar, 99.99%), Nd_2O_3 (Alfa Aesar, 99.99%), and NiO (Sigma Aldrich-Chemie GmbH, 99.995%) prepared by a solid-state reaction in air at 1100 ℃ for 24 hours. The products of this reaction were ground and reheated, and this process was repeated five times. The resulting polycrystalline materials was pressed into a pellet and sintered for 24 hours at 1200 ℃ in air. The heating and cooling rate of the sintering were kept at 3 ℃/min.

The nickelate films were grown by PLD using a 248-nm KrF excimer laser (COMPex 201, Coherent). The $SrTiO_3$ (001) substrates (5×5 mm, without chem-

Supported in part by the National Natural Science Foundation of China (Grant Nos. 12074411 and 11888101), the National Key Research and Development Program of China (Grant Nos. 2016YFA0300300 and 2017YFA0302900), the Strategic Priority Research Program (B) of the Chinese Academy of Sciences (Grant No. XDB25000000), and the Research Program of Beijing Academy of Quantum Information Sciences (Grant No. Y18G06).
*Corresponding authors. Email: XJZhou@iphy.ac.cn; zzh@iphy.ac.cn
© 2021 Chinese Physical Society and IOP Publishing Ltd

ical etching to achieve a TiO_2 terminated surface) were pre-annealed at 900 ℃ with an oxygen partial pressure of 1×10^{-5} Torr. During growth, the substrate temperature was kept at 600 ℃ under an oxygen partial pressure of 150 mTorr. After deposition, the films were cooled to room temperature at a rate of 5 ℃ per minute in the same oxygen partial pressure. The laser beam size was about $0.8 \times 3.2\,mm^2$ realized by using an aperture. The pulse energy of the laser was set from $640\,mJ/cm^2$ to $960\,mJ/cm^2$ for the growth of $NdNiO_3$ and $Nd_{0.8}Sr_{0.2}NiO_3$. The laser frequency was set to 4 Hz.

The infinite-layer nickelate phase was acquired by the soft-chemistry reduction method. As shown in Fig. 1(b), the as-grown nickelate films were wrapped in clean aluminum foil and then sealed with 0.1 g CaH_2 powder (Alfa Aesar, 98%) in quartz tubes which were pumped to a vacuum better than 1×10^{-5} Torr. The reduction was carried out at a temperature of 290 ℃ for 5 hours, with the heating and cooling rates of 10 ℃/min.

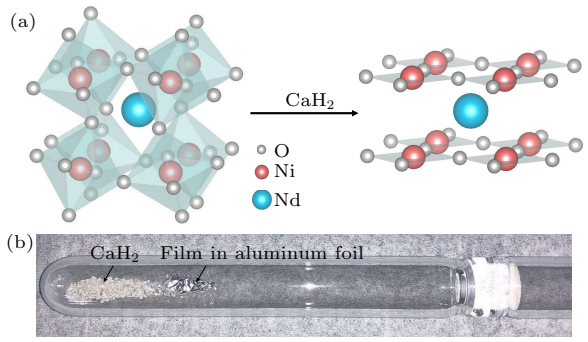

Fig. 1. Crystal structure and the reduction process of nickelates. (a) Illustration of the crystal structures of $NdNiO_3$ (left) and $NdNiO_2$ (right). (b) The soft-chemistry reduction process. A typical $Nd_{0.8}Sr_{0.2}NiO_3$ film wrapped in aluminum foil is vacuum-sealed with CaH_2 powder in a quartz tube.

Figure 2 shows the structural characterization of the nickelate films. The $NdNiO_3$ film peaks at 23.76° and 48.56° correspond to the (001) and (002) reflections, respectively [see Fig. 2(a)]. After chemical reduction, as shown in Fig. 2(b) the film peaks at 26.77° and 55.85° identify the infinite-layer $NdNiO_2$ and correspond to (001) and (002) reflections, respectively. For a typical film of $Nd_{0.8}Sr_{0.2}NiO_3$ shown in Fig. 2(c), the peaks at 23.75° and 48.45° correspond to (001) and (002) reflections, respectively, and both peaks are slightly broader than those of the undoped phase in Fig. 2(a). After chemical reduction, the peaks at 26.45° and 54.77° correspond to (001) and (002) reflections, respectively, as expected for a film of an infinite-layer $Nd_{0.8}Sr_{0.2}NiO_2$ [Fig. 2(d)]. The intensity is comparable to the precursor. It was reported that the $Nd_{0.8}Sr_{0.2}NiO_3$ films were difficult to grow due to the formation of a secondary phase which shows only a single peak with 2θ less than 48°.[52]

In Fig. 3 we show the measured $Nd_{0.8}Sr_{0.2}NiO_2$ film resistance as a function of temperature revealing that a superconducting transition occurs below 9 K and the zero resistivity is achieved at about 3.5 K. The superconducting transition temperature of our film is slightly lower than that reported in the literature, which probably stems from the variation of the hole concentration in the films prepared under differing growth and reduction conditions. To study the stability of the superconducting $Nd_{0.8}Sr_{0.2}NiO_2$ films, we measured the resistivity of a typical film which had been kept in the glovebox for 30 days after chemical reduction and had been exposed to air longer than 10 hours during XRD and other measurements. The fact that the superconducting transition is almost identical with the same critical temperature T_c, as shown in Fig. 3(c), implies that the 9-nm-thick superconducting film without a capping layer is fairly stable.

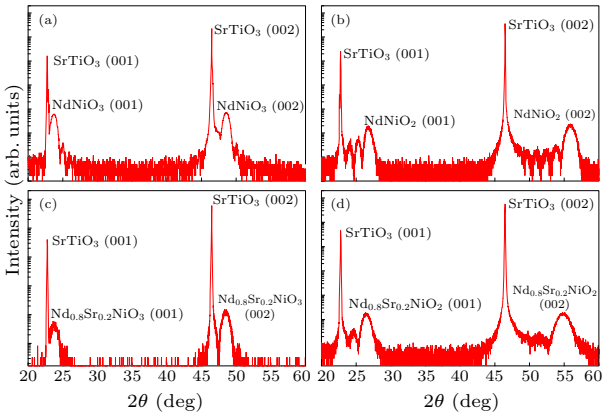

Fig. 2. Structural characterization of nickelate films on STO substrates. (a) The XRD θ–2θ scans of a typical $NdNiO_3$ film with a thickness of 10 nm. (b) The XRD θ–2θ scans of the infinite-layer $NdNiO_2$ film acquired by performing topotactic reduction on the sample (a) at 290 ℃ for 5 hours. (c) The XRD θ–2θ scans of a typical $Nd_{0.8}Sr_{0.2}NiO_3$ film with a thickness of 9 nm. (d) The XRD θ–2θ scans of the infinite-layer $Nd_{0.8}Sr_{0.2}NiO_2$ film acquired by reducing the sample (c) at 290 ℃ for 5 hours.

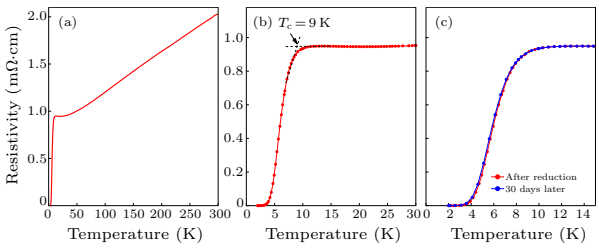

Fig. 3. Transport properties of $Nd_{0.8}Sr_{0.2}NiO_2$ thin film. (a) Temperature-dependent resistivity of the $Nd_{0.8}Sr_{0.2}NiO_2$ thin film from 300 K to 2 K. (b) A zoom-in view of (a) with the temperature lower than 30 K. The onset of the superconducting transition is about 9 K. (c) An aging test of a nickelate superconducting film. The transport measurement shows almost identical superconducting transition, over a period of 30 days after the topotactic reduction.

The growth window is extremely narrow probably because the formation energy of the desired 113 phase differs only slightly from that of the secondary phase. Nevertheless, we find that the XRD pattern

of the precursor 113 phase is a good criterion to obtain superconducting films. The (002) peak of the secondary phase locates at about 47.8°, while for the 113 phase the (002) peak is at the 2θ larger than 48° and thickness-dependent. During the optimization, we adjusted the laser spot size and laser pulse energy with the growth temperature at 600 ℃ and an oxygen partial pressure of 150 mTorr unchanged, and keep the thickness at 8 nm to 10 nm. The out-plane XRD pattern of a typical film grown with a larger laser spot size of $1.5\times5.0\,\mathrm{mm}^2$ is shown in Fig. 4(a). The fact that the location of the (002) peak at 47.8° and a weak hump of the (001) reflection indicates that the film contains both the 113 phase and the secondary phase. After reduction [Fig. 4(b), black curve], infinite-layer phase were partly achieved as the XRD pattern is weaker and smaller than the film of Fig. 2(d). The transport measurement shows an insulating behavior at low temperature. In Fig. 4(c) we show the XRD patterns around the (002) reflection for the films grown still with the large spot size but by using different pulse energy from $600\,\mathrm{mJ/cm}^2$ to $1200\,\mathrm{mJ/cm}^2$, and the 2θ of the (002) peaks is always less than 48°. Figures 4(a), 4(b), and 4(d) plot the XRD patterns for the films grown using a smaller laser spot size of $0.8\times3.2\,\mathrm{mm}^2$ with an optical aperture and different pulse energy, for which the variation of the 2θ of the (002) reflection from 48.0° to 48.4° and the appearance of the (001) peak reflect a competition between the secondary phase and the desired 113 phase. As shown in Figs. 4(a) and 4(b), the precursor film with a higher concentration of the 113 phase than the secondary phase tends to be reduced to the infinite-layer phase with a larger 2θ for the (002) peak, and it is more likely a superconducting one at low temperature [see Fig. 4(e)]. With the criterion of the (002) peak position, we found that the best laser pulse energy window is from 800 to $960\,\mathrm{mJ/cm}^2$, and we manage to produce at least one superconducting sample out of the ten films under such conditions [Fig. 4(d)]. From our results, the laser spot size and pulse energy are two key factors to reduce the secondary phase and to improve the reproducibility of superconducting films.

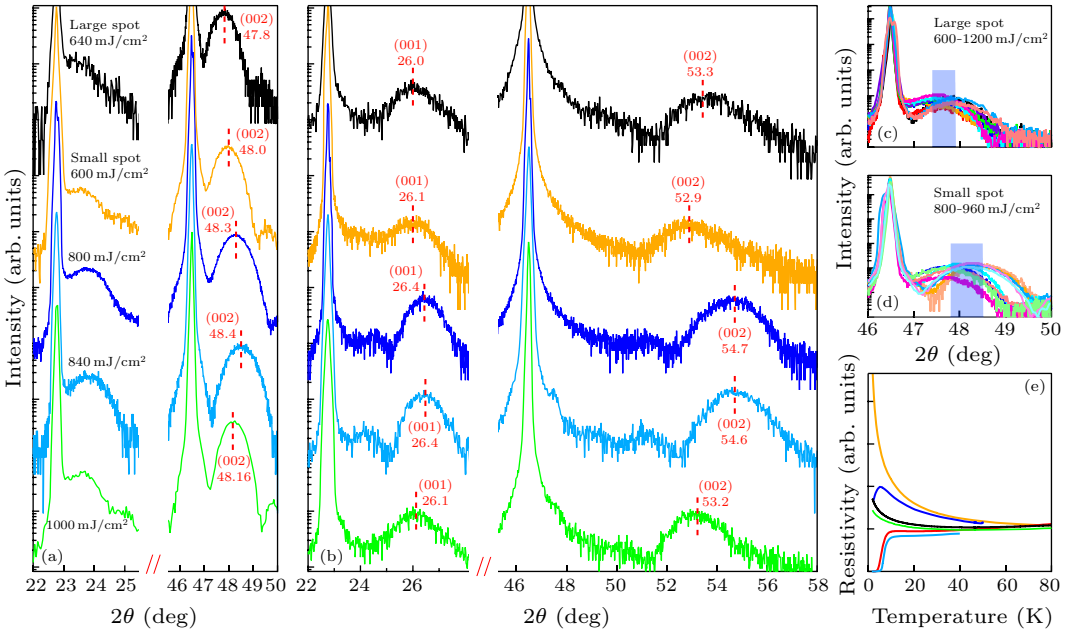

Fig. 4. Optimization of the growth condition of $Nd_{0.8}Sr_{0.2}NiO_3$ thin film. (a) The XRD θ–2θ scans of typical $Nd_{0.8}Sr_{0.2}NiO_3$ films grown with a large laser spot of $1.5\times5.0\,\mathrm{mm}^2$ (black line) and a small laser spot of $0.8\times3.2\,\mathrm{mm}^2$ (yellow, blue, sky blue, green lines) under different laser pulse energy. (b) The XRD θ–2θ scans of the film acquired by reducing the samples of (a) at 290 ℃ by five hours. The data in (a) and (b) are offset for clarity. (c) The XRD θ–2θ scans of $Nd_{0.8}Sr_{0.2}NiO_3$ films grown with a large laser spot and different pulse energy. (d) The XRD θ–2θ scans of $Nd_{0.8}Sr_{0.2}NiO_3$ films grown with a small laser spot and different pulse energy. The blue boxes in (c) and (d) mark the locations of (002) peak. (e) Temperature-dependent resistivity of the films of (b). The red one is from Fig. 3(a). The results are normalized at high temperature for comparison. The thickness of all the films are about 9 nm (±1 nm).

The reduction process is relatively straightforward if the pure 113 phase is achieved. In Fig. 5(a) we show the out-plane XRD pattern of a typical $NdNiO_3$ film, which consists of both the 113 phase and the secondary phase. After the reduction, the peak from the secondary phase moves to the smaller 2θ angle, while the (002) peak of the 113 phase moves to the larger 2θ angle, representing the transformation from the 113 perovskite phase to the infinite-layer phase. For a pure sample, we varied the annealing temperature with the annealing time fixed to 5 hours. In our case, we found that the temperature of 290 ℃ is a good reduction condition to achieve the infinite-layer phase [Figs. 5(d)–5(f)].

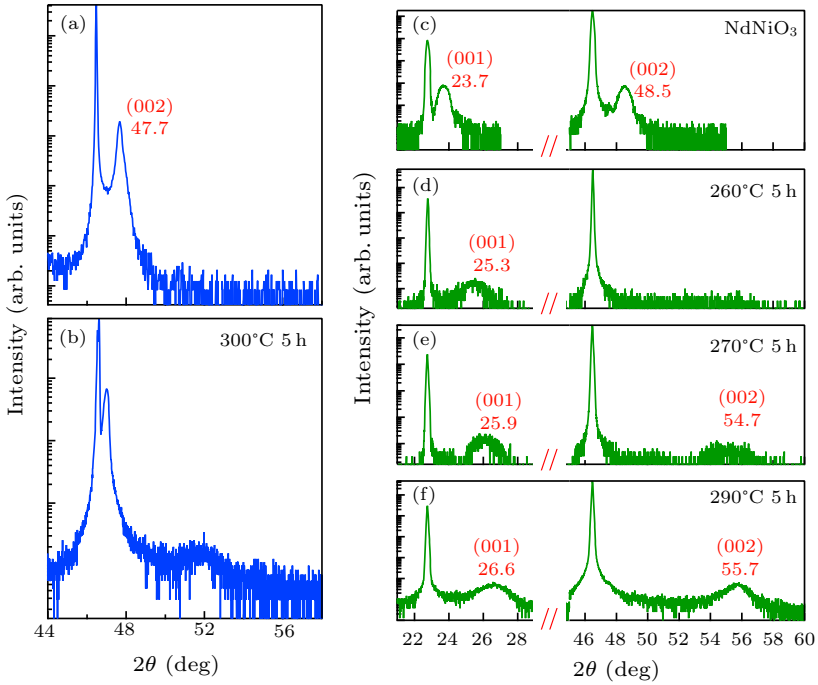

Fig. 5. Reduction process of $NdNiO_3$ thin films. (a) The XRD θ–2θ scans of a $NdNiO_3$ film which is dominated by the secondary phase. (b) The XRD θ–2θ scans of the reduced film of (a). (c) The XRD θ–2θ scans of a high-quality $NdNiO_3$ film. (d)–(e) The XRD θ–2θ scans of the reduced films with comparable quality to that of the sample in (c) under different temperatures.

In summary, we have successfully synthesized superconducting infinite-layer $Nd_{0.8}Sr_{0.2}NiO_2$ thin films using pulsed laser deposition and the soft-chemistry reduction method. The details on the film growth and the subsequent topotactic reduction process are discussed. Our results provide important information for the preparation of superconducting nickelate films, which is a crucial step in this field.

Acknowledgement. We wish to thank Er-jia Guo for helpful discussions.

References

[1] Chaloupka J and Khaliullin G 2008 *Phys. Rev. Lett.* **100** 016404
[2] Boris A *et al.* 2011 *Science* **332** 937
[3] Li D *et al.* 2019 *Nature* **572** 624
[4] Li D *et al.* 2020 *Phys. Rev. Lett.* **125** 027001
[5] Zeng S *et al.* 2020 *Phys. Rev. Lett.* **125** 147003
[6] Osada M *et al.* 2020 *Phys. Rev. Mater.* **4** 121801
[7] Hepting M *et al.* 2020 *Nat. Mater.* **19** 381
[8] Goodge B *et al.* 2021 *Proc. Natl. Acad. Sci. USA* **118** e2007683118
[9] Rossi M *et al.* 2020 arXiv:2011.00595 [cond-mat.str-el]
[10] Hayward M and Rosseinsky M 2003 *Solid State Sci.* **5** 839
[11] Botana A and Norman M 2020 *Phys. Rev. X* **10** 011024
[12] Hirsch J and Marsiglio F 2019 *Physica C* **566** 1353534
[13] Jiang P *et al.* 2019 *Phys. Rev. B* **100** 201106
[14] Nomura Y *et al.* 2019 *Phys. Rev. B* **100** 205138
[15] Zhang G *et al.* 2019 *Phys. Rev. B* **100** 020501
[16] Adhikary P *et al.* 2020 *Phys. Rev. B* **102** 100501
[17] Karp J *et al.* 2020 *Phys. Rev. X* **10** 021061
[18] Bandyopadhyay S *et al.* 2020 *Phys. Rev. B* **102** 220502
[19] Chang J *et al.* 2020 *Eur. Phys. J. B* **93** 220
[20] Choi M *et al.* 2020 *Phys. Rev. B* **101** 020503
[21] Geisler B and Pentcheva R 2020 *Phys. Rev. B* **102** 020502
[22] Gu Y *et al.* 2021 *Chin. Phys. Lett.* **38** 017501
[23] Gu Y *et al.* 2020 *Commun. Phys.* **3** 1
[24] He R *et al.* 2020 *Phys. Rev. B* **102** 035118
[25] Ji C *et al.* 2020 *Phys. Rev. Mater.* **4** 124804
[26] Jiang M *et al.* 2020 *Phys. Rev. Lett.* **124** 207004
[27] Kapeghian J and Botana A 2020 *Phys. Rev. B* **102** 205130
[28] Katukur V *et al.* 2020 *Phys. Rev. B* **102** 241112
[29] Krishna J *et al.* 2020 *Phys. Rev. B* **102** 224506
[30] Lang Z J *et al.* 2021 *Phys. Rev. B* **103** L180502
[31] Gao J C *et al.* 2020 *Natl. Sci. Rev.* nwaa218
[32] Lechermann F 2020 *Phys. Rev. X* **10** 041002
[33] Lechermann F 2020 *Phys. Rev. B* **101** 081110
[34] Leonov I *et al.* 2020 *Phys. Rev. B* **101** 241108
[35] Liu Z *et al.* 2020 *npj Quantum Mater.* **5** 31
[36] Nica E *et al.* 2020 *Phys. Rev. B* **102** 020504
[37] Petocchi F *et al.* 2020 *Phys. Rev. X* **4** 041047
[38] Ryee S *et al.* 2020 *Phys. Rev. B* **101** 064513
[39] Sakakibara H *et al.* 2020 *Phys. Rev. Lett.* **125** 077003
[40] Si L *et al.* 2020 *Phys. Rev. Lett.* **124** 166402
[41] Wang Y *et al.* 2020 *Phys. Rev. B* **102** 161118
[42] Wang Z *et al.* 2020 *Phys. Rev. B* **102** 220501
[43] Werner P and Hoshino S 2020 *Phys. Rev. B* **101** 041104
[44] Wu X *et al.* 2020 *Phys. Rev. B* **101** 060504
[45] Wu X *et al.* 2020 arXiv:2008.06009 [cond-mat.supr-con]
[46] Zhang R *et al.* 2021 *Commun. Phys.* **4** 118
[47] Zhang Y *et al.* 2020 *Phys. Rev. B* **102** 195117
[48] Klett M *et al.* 2021 arXiv:2101.04689 [cond-mat.supr-con]
[49] Liu Z *et al.* 2021 *Phys. Rev. B* **103** 045103
[50] Wan X *et al.* 2021 *Phys. Rev. B* **103** 075123
[51] Osada M *et al.* 2020 *Nano Lett.* **20** 5735
[52] Lee K *et al.* 2020 *APL Mater.* **8** 041107
[53] Gu Q *et al.* 2020 *Nat. Commun.* **11** 6027
[54] Xiang Y *et al.* 2021 *Chin. Phys. Lett.* **38** 047401
[55] Wang B *et al.* 2021 *Nat. Phys.* **17** 473
[56] Zhou X *et al.* 2020 *Rare Met.* **39** 368
[57] Li Q *et al.* 2020 *Commun. Mater.* **1** 16
[58] Wang B *et al.* 2020 *Phys. Rev. Mater.* **4** 084409
[59] He C *et al.* 2020 arXiv:2010.11777 [cond-mat.supr-con]
[60] Cui Y *et al.* 2021 *Chin. Phys. Lett.* **38** 067401